Published in final edited form as:
Nature. 2005 May 19; 435(7040): 365–369.

Non-equilibration of hydrostatic pressure in blebbing cells

Guillaume T. Charras[1], **Justin C Yarrow**[1], **Mike A. Horton**[2], **L. Mahadevan**[1,3,4], and **T.J. Mitchison**[1]

1*Department of Systems Biology, Harvard Medical School, Boston, MA, USA*

2*London Centre for Nanotechnology, University College London, London, UK*

3*Division of Engineering and Applied Sciences, Harvard University, Cambridge, MA, USA*

4*Department of Organismic and Evolutionary Biology, Harvard University, Cambridge, MA, USA*

Letter to Nature

Current models for protrusive motility in animal cells focus on cytoskeleton-based mechanisms, where localized protrusion is driven by local regulation of actin biochemistry[1–3]. In plants and fungi, protrusion is driven primarily by hydrostatic pressure[4–6]. For hydrostatic pressure to drive localized protrusion in animal cells[7,8], it would have to be locally regulated, but current models treating cytoplasm as an incompressible viscoelastic continuum[9] or viscous liquid[10] require that hydrostatic pressure equilibrates essentially instantaneously over the whole cell. Here, we use cell blebs as reporters of local pressure in the cytoplasm. When we locally perfuse blebbing cells with cortex-relaxing drugs to dissipate pressure on one side, blebbing continues on the untreated side, implying non-equilibration of pressure on scales of ~10μm and ~10sec. We can account for localization of pressure by considering the cytoplasm as a contractile, elastic network infiltrated by cytosol. Motion of the fluid relative to the network generates spatially heterogenous transients in the pressure field, and can be described in the framework of poroelasticity[11,12].

Blebs are large, approximately spherical deformations of the cell surface that form and disappear on a time-scale of tens of seconds. Though less studied than lamellipodial or filopodial protrusion, blebbing is a common phenomenon during apoptosis[13], cytokinesis[14,15] and cell movement[16,17]. Blebs are thought to be initiated by rupture of the plasma membrane from the underlying cytoskeleton (Supplementary figure S3), followed by inflation of the detached membrane by intracellular fluid flow[18,19]. Subsequent bleb retraction is driven by assembly and contraction of a cortex within the newly formed bleb. Blebbing requires non-uniform behaviour of the membrane and cortex, that must reflect either a globally uniform hydrostatic pressure combined with local nucleation of membrane detachment from the cytoskeleton, or non-uniform pressure leading to local rupture of membrane-cytoskeleton attachments in regions of high pressure. To distinguish these possibilities, we studied the effect of local disruption of cortical contraction or integrity induced by drug perfusion over part of a cell, in a filamin-depleted melanoma cell line (M2) that blebs extensively and continuously[20].

We first confirmed that the cell volume stays approximately constant during blebbing (Supplementary data, video S12 and figure S4)[18], implying that blebbing is driven primarily

Corresponding author: Guillaume Charras, Dept of Systems Biology, HMS, 250 Longwood Avenue, Boston, MA 02115, Email:gcharras@hms.harvard.edu, Tel: 1-617-432-3724; Fax: 1-617-432-3442.

Competing interests and materials request statements
The authors declare they have no competing financial interests.

Correspondence and requests should be addressed to Guillaume Charras:gcharras@hms.harvard.edu

More methods, results and theory are available online as supplementary information.

by flow of fluid within the cell rather than water crossing the plasma membrane. We then confirmed that bleb inflation represents ballooning out of the plasma membrane when it detaches from the actin cortex by simultaneously imaging the cortex and the cell membrane (Supplementary figure S3). During bleb inflation, GFP-actin was not enriched at the bleb surface compared to its interior, implying lack of a cytoskeleton in the bleb (Figure 1A, t=0,22s). As inflation slowed, a cortical cytoskeleton assembled underneath the bleb membrane, evidenced by a rim of actin fluorescence (Figure 1A, t=62s); simultaneously, the cortex at the base of the bleb dissassembled (Supplementary figure S3). As the bleb retracted, its actin rim became more pronounced, and often wavy or buckled, suggesting that the cortex contracts as the bleb shrinks (Figure 1A, t= 72s)[19]. GFP-myosin II regulatory light chain (MRLC) was recruited to the newly forming cortex of the bleb simultaneous with actin (Figure 1B, Supplementary video 10)[13,21], consistent with myosin II driving contraction. Increasing extracellular osmolarity made blebs smaller, and decreasing it made them larger[22] (Supplementary Video 1 and Figure 1). Increasing membrane rigidity by crosslinking the glycocalix polysaccharides with Wheat Germ Agglutinin (WGA)[23] inhibits blebbing (Supplementary Video 2). These observations, together with drug studies discussed below, support the following qualitative model for bleb dynamics[19]. Cortical acto-myosin contracts (Supplementary video 10 and 11), generating hydrostatic pressure that causes a patch of plasma membrane to tear free from its attachment to the cortical cytoskeleton. This patch of cytoskeleton-free membrane rapidly inflates as cytosol flows in, with its base enlarging by further tearing (Supplementary figure S3). Later, inflation slows and a mesh of actin and myosin II assembles in the bleb to form a contractile cortex attached to the plasma membrane (Figure 1B). Finally, contraction of this cortical mesh causes the bleb to shrink, driving the extruded cytosol back into the cell body.

To find small molecule tools, we screened a library of known bioactive compounds for rapid inhibition of blebbing[24]. After characterizing their effects in bath treatment, selected drugs and osmolytes were applied locally to cells by injecting medium containing inhibitor via a micropipette into a laminar fluid flow[24–26]. The treated region was visualized by adding a fluorescent tracer to the pipette medium, while blebbing was observed using DIC microscopy. During local perfusion, we typically bathed 20–33% of the cell area. We confirmed local application by visualizing local deposition of a fluorescent lectin (WGA-Alexa 488; Figure 2A, t=430s). For each drug, local perfusion experiments were repeated until one of the following behaviors was observed reproducibly ($N \geq 5$): (i) local perfusion of drug inhibited blebbing locally, (ii) local perfusion had both a local and global effect on blebbing, (iii) local perfusion did not inhibit blebbing but whole cell treatment did.

The effect of local perfusion could be classified into three categories: (i) Treatments that locally inhibited blebbing, but allowed the untreated part of the cell to bleb normally (Figure 2, Supplementary Table 1, Supplementary Videos 3–6). As expected, agents that increased membrane rigidity (WGA) or osmotic pressure (sucrose) had this effect (Figures 2A–B). These agents locally increase the physical forces that oppose blebbing. More surprising, drugs that block generation of contractile force also inhibited locally, including inhibitors of myosin II (blebbistatin21) and ROCK1 (Y-27632 and 3-(4-pyridyl)indole[27]), a kinase that activates myosin II (Figures 2C–D). (ii) Treatments that caused a combination of local and global effects, as seen with the F-actin disrupting agents Cytochalasin D and Latrunculin B (Figure 3A, Supplementary Video 7). Within seconds of local drug application, there was a global increase in bleb size (Figure 3A, t=75s).Then, blebbing ceased in the treated area and existing blebs were not retracted, while blebbing continued in the untreated area at a slower rate than pre-drug (Figure 3A, t=315s). (iii) Treatments that only had an effect when the whole cell was treated. Inhibitors of several other protein kinases had this effect (Figures 3B–C, Supplementary Videos 8–9). For local perfusion to locally perturb the cytoplasm, membrane crossing must be fast compared to intracellular diffusion of the drug or drug-target

complex[28]. Thus, failure to see a local effect of a drug cannot be interpreted in terms of local versus global action of its target.

The local effects of myosin II inhibiting drugs (Figures 2C–D) show that the acto-myosin cortex acts locally to promote blebbing. This could be because contraction locally nucleates blebs, while hydrostatic pressure is uniform, or because pressure generated by contraction only acts locally to extrude blebs, implying it does not globally equilibrate. Local inhibition of blebbing by actin depolymerising drugs (Figure 3A) favors the latter hypothesis. If pressure equilibrated across the cell, the drug-treated side, where the cortex is softer, should swell preferentially, inhibiting blebbing on the untreated side. Since this does not happen, we conclude that hydrostatic pressure does not equilibrate across single M2 cells on time- and length-scales relevant to motility.

Current models of the cytoplasm[9,10] cannot account for spatio-temporally localized variations in hydrostatic pressure. We therefore propose a new description of the cytoplasm based on the poroelasticity[11,12]. We consider the cytoplasm as composed of a porous, actively contractile, elastic network (cytoskeletal filaments, organelles, and ribosomes), infiltrated with an interstitial fluid (cytosol: water, ions and soluble proteins), similar to a fluid-filled sponge. Contraction of the acto-myosin cortex creates a compressive stress on the cytoskeletal network, leading to a spatially localized increase in hydrostatic pressure (Figure 4A). In response, the cytosol flows out of the network, and if it finds a region where the membrane is weakly attached to the cortex, the resulting pressure can lead to membrane detachment and bleb inflation (Figure 4B, Supplementary figure S3). With a poroelastic description of the cytoplasm, hyrdostatic pressure does not instantaneously propagate through the network. Instead, it diffuses over a length $x \approx \sqrt{Dt}$ during a time *t*, with the diffusion constant $D = \frac{kK}{\varphi}$ determined by an appropriately defined elastic bulk modulus K, the hydraulic permeability of the network k, and the local volume fraction of fluid φ (see supplementary theory). The diffusion constant D dictates the time needed for the effect of a local contractile force to be felt in other parts of the cell. Using a typical time-scale for bleb inflation of *t*~10s and realistic values for the various parameters (Supplementary theory), we find *x*~15–30 μm. Hence, hydrostatic pressure can be strongly non-equilibrated in cells on a time-scale of ~10s and a length-scale of ~10 μm: scales that are relevant to a variety of motile behaviors. Bleb formation reduces this length-scale by allowing the fluid to flow, with less resistance, into the blebs instead of through the network. Local inhibition of blebbing is possible because opposite sides of the cells are effectively isolated from each other with respect to equilibration of pressure on a time scale of seconds.

Our poroelastic model could have important implications for other types of cell motility, since it implies that hydrostatic pressure can be generated and used locally to power shape change in animal cells. Leading edge protrusion is typically coupled to actin polymerisation [1–3], but hydrodynamic force could work together with polymerization force to power protrusion[7,8], and fluid flow could drive actin subunits forwards at a faster rate than that predicted by pure diffusion[29]. Localized hydrostatic pressure transients could be generated locally near the front of polarised cells by local recruitment and activation of myosin II as in blebbing, or of plasma membrane ion transporters (such as NHE1[30]) that can trigger swelling through influx of an osmolyte (such as Na^+). Overall, our work shows that cytosolic fluid dynamics must be integrated with protein dynamics if we are to really understand cell motility.

Methods

Local Perfusion

Local perfusion was performed by injecting medium with the desired concentration of drug into a laminar fluid flow via a glass micropipette with a 1–2 μm diameter. Thin walled

borosilicate micropipettes (0.9 mm inner diameter) were pulled on a Sutter P87 pipette puller (Sutter instrument company). Coverslips on which cells had been cultured were affixed onto the bottom of the laminar fluid flow chamber (blueprint available upon request) with a 1:1:1 mix of vaseline, lanolin and paraffin. Laminar flow was created by feeding medium into the flow chamber at a constant rate of 30 $ml.h^{-1}$ with a syringe pump. A constant fluid level was maintained by aspirating the supernatant via a vacuum pump. The flow chamber consisted of a reservoir with a small opening (0.7 mm) that enables medium to enter the open part of the chamber and delivers a flow of approximately 30 $\mu m.s^{-1}$ in the vicinity of this entrance. For the flow to be sufficiently rapid to carry drug away, the target cells needed to be chosen within 200 μm of the reservoir opening. All experiments were performed at room temperature in Leibovitz-L15 medium with 10% 80:20 mix of donor calf serum:foetal calf serum. The microinjected solution was made up of medium with the desired concentration of drug and 0.1μM of Tetramethylrhodamine (used as a fluorescent tracer) and filtered using a centrivac tube (Millipore corporation, Billerica, MA). The micropipettes were backfilled with the solution and mounted onto a pipette holder attached to a three axis oil hydraulic micromanipulator (Narishige, Tokyo, Japan). A pressure regulator (Eppendorf 5242, Eppendorf AG, Hamburg, Germany) set between 40 and 80 hPa was used to control flow from the micropipette.

Time-lapse video-microscopy of the local perfusion experiments was performed as described in supplementary methods except that in addition to DIC images, fluorescence images were also acquired (TRITC filters to visualise flow lines and FITC filters to visualise WGA-Alexa 488). Exposure times were ~200 ms for DIC images, ~600 ms for TRITC images, and ~250ms for FITC images. Images were acquired every 5s with a 20x objective. During a typical local perfusion experiment, ~30 images (~150s) were acquired prior to drug exposure. Then, the cell was exposed to drug for ~70 images (~350s), finally the cell was allowed to recover for 20 frames (~100s). When no local inhibition was observed, a whole cell treatment was performed. This time, the cell was observed for 30 frames to ensure that it still blebbed, the whole cell was exposed to drug for 70 frames, and recovered for 20 frames. Initial concentrations of drug in the microinjected fluid were chosen to be 2-3x those needed in bulk solution. When no inhibition was observed when the whole cell was exposed to drug, the drug concentration in the micropipette was increased. When whole cell inhibition was observed with only local perfusion, the drug concentration was decreased.

Post-hoc, flow lines were superimposed onto the DIC images using metamorph. The fluorescence images were thresholded and intensities of 25% of the maximum intensity were converted to a binary image that was inverted and superimposed onto the DIC image using an AND operator.

Analysis and Quantitation of Local Perfusion Assays

Each cell was divided into two regions: the treated region where local perfusion was applied and the control untreated region. Each experiment was divided into different periods: 1) prior to the application of drug, 2) during local application of drug, 3) after application of drug, and, if need be, 4) during whole cell treatment. The number of blebs occuring in each region for each period was counted manually. A blebbing index was computed for each region as follows: $B = \frac{N_{blebs}}{Lt}$ with N_{blebs} the number of blebs observed during a given period t over a given perimeter L. These blebbing indices were used to compare the treated region to the untreated region prior to application of inhibitor, and the blebbing in either region during and after application of inhibitor to the blebbing in that region prior to application. Populations were compared with a Student t-test and the level of significance was taken to be $p<0.01$. For graphic output (Figures 2 and 3), the evolution of the blebbing indices were normalised to their values

prior to application of local perfusion. In all cases, the blebbing index in the treated and untreated region were not significantly different prior to application of inhibitor ($p>0.3$).

Supplementary Material

Refer to Web version on PubMed Central for supplementary material.

Acknowledgements

The authors would like to acknowledge the Nikon Imaging Centre at Harvard Medical School and, in particular, Jennifer Waters. The authors would also like to acknowledge Jim Horn at the HMS machine shop for manufacturing the perfusion chamber. GTC was in receipt of Wellcome Trust Overseas Fellowship GR068264AIA. MAH is supported by a Program Grant from the Wellcome Trust. LM was supported by NSF-MRSEC at Harvard University. This work was supported by NIH-GM 48027.

References

1. Mahadevan L, Matsudaira P. Motility powered by supramolecular springs and ratchets. Science 2000;288:95–100. [PubMed: 10753126]
2. Rafelski SM, Theriot JA. Crawling toward a unified model of cell mobility: spatial and temporal regulation of actin dynamics. Annu Rev Biochem 2004;73:209–39. [PubMed: 15189141]
3. Mogilner A, Oster G. Polymer motors: pushing out the front and pulling up the back. Curr Biol 2003;13:R721–33. [PubMed: 13678614]
4. Messerli MA, Robinson KR. Ionic and osmotic disruptions of the lily pollen tube oscillator: testing proposed models. Planta 2003;217:147–57. [PubMed: 12721859]
5. Money NP, Harold FM. Extension growth of the water mold Achlya: interplay of turgor and wall strength. Proc Natl Acad Sci U S A 1992;89:4245–9. [PubMed: 11607292]
6. Harold FM. Force and compliance: rethinking morphogenesis in walled cells. Fungal Genet Biol 2002;37:271–82. [PubMed: 12431461]
7. Tilney LG, Inoue S. Acrosomal reaction of the Thyone sperm. III. The relationship between actin assembly and water influx during the extension of the acrosomal process. J Cell Biol 1985;100:1273–83. [PubMed: 3920226]
8. Condeelis J. Life at the leading edge: the formation of cell protrusions. Annu Rev Cell Biol 1993;9:411–44. [PubMed: 8280467]
9. Boal, D. H. *Mechanics of the cell* (Cambridge University Press, 2002).
10. Drury JL, Dembo M. Hydrodynamics of micropipette aspiration. Biophys J 1999;76:110–28. [PubMed: 9876128]
11. Biot M. General Theory of Three-dimensional Consolidation. J Appl Phys 1941;12:155–164.
12. Wang, H. *Theory of Linear Poroelasticity with Applications to Geomechanics and Hydrogeology* (Princeton University Press, 2000).
13. Mills JC, Stone NL, Erhardt J, Pittman RN. Apoptotic membrane blebbing is regulated by myosin light chain phosphorylation. J Cell Biol 1998;140:627–36. [PubMed: 9456322]
14. Fishkind DJ, Cao LG, Wang YL. Microinjection of the catalytic fragment of myosin light chain kinase into dividing cells: effects on mitosis and cytokinesis. J Cell Biol 1991;114:967–75. [PubMed: 1874791]
15. Burton K, Taylor DL. Traction forces of cytokinesis measured with optically modified elastic substrata. Nature 1997;385:450–4. [PubMed: 9009194]
16. Trinkaus JP. Surface activity and locomotion of Fundulus deep cells during blastula and gastrula stages. Dev Biol 1973;30:69–103. [PubMed: 4735370]
17. Friedl P, Wolf K. Tumour-cell invasion and migration: diversity and escape mechanisms. Nat Rev Cancer 2003;3:362–74. [PubMed: 12724734]
18. Albrecht-Buehler G. Does blebbing reveal the convulsive flow of liquid and solutes through the cytoplasmic meshwork? Cold Spring Harb Symp Quant Biol 46 Pt 1982;1:45–9.
19. Cunningham CC. Actin polymerization and intracellular solvent flow in cell surface blebbing. J Cell Biol 1995;129:1589–99. [PubMed: 7790356]

20. Cunningham CC, et al. Actin-binding protein requirement for cortical stability and efficient locomotion. Science 1992;255:325–7. [PubMed: 1549777]
21. Cheung A, et al. A small-molecule inhibitor of skeletal muscle myosin II. Nat Cell Biol 2002;4:83–8. [PubMed: 11744924]
22. Dai J, Sheetz MP. Membrane tether formation from blebbing cells. Biophys J 1999;77:3363–70. [PubMed: 10585959]
23. Evans E, Leung A. Adhesivity and rigidity of erythrocyte membrane in relation to wheat germ agglutinin binding. J Cell Biol 1984;98:1201–8. [PubMed: 6546931]
24. Materials. *Materials and methods are available as supporting material on Science Online.*
25. Popov S, Brown A, Poo MM. Forward plasma membrane flow in growing nerve processes. Science 1993;259:244–6. [PubMed: 7678471]
26. O'Connell CB, Warner AK, Wang Y. Distinct roles of the equatorial and polar cortices in the cleavage of adherent cells. Curr Biol 2001;11:702–7. [PubMed: 11369234]
27. Yarrow, J. C., Totsukawa, G., Charras, G. T. & Mitchison, T. J. Screening for cell migration inhibitors using automated microscopy reveals a new rho-kinase inhibitor. *Manuscript in preparation* (2004).
28. Takayama S, et al. Selective chemical treatment of cellular microdomains using multiple laminar streams. Chem Biol 2003;10:123–30. [PubMed: 12618184]
29. Zicha D, et al. Rapid actin transport during cell protrusion. Science 2003;300:142–5. [PubMed: 12677069]
30. Baumgartner M, Patel H, Barber DL. Na(+)/H(+) exchanger NHE1 as plasma membrane scaffold in the assembly of signaling complexes. Am J Physiol Cell Physiol 2004;287:C844–50. [PubMed: 15355855]

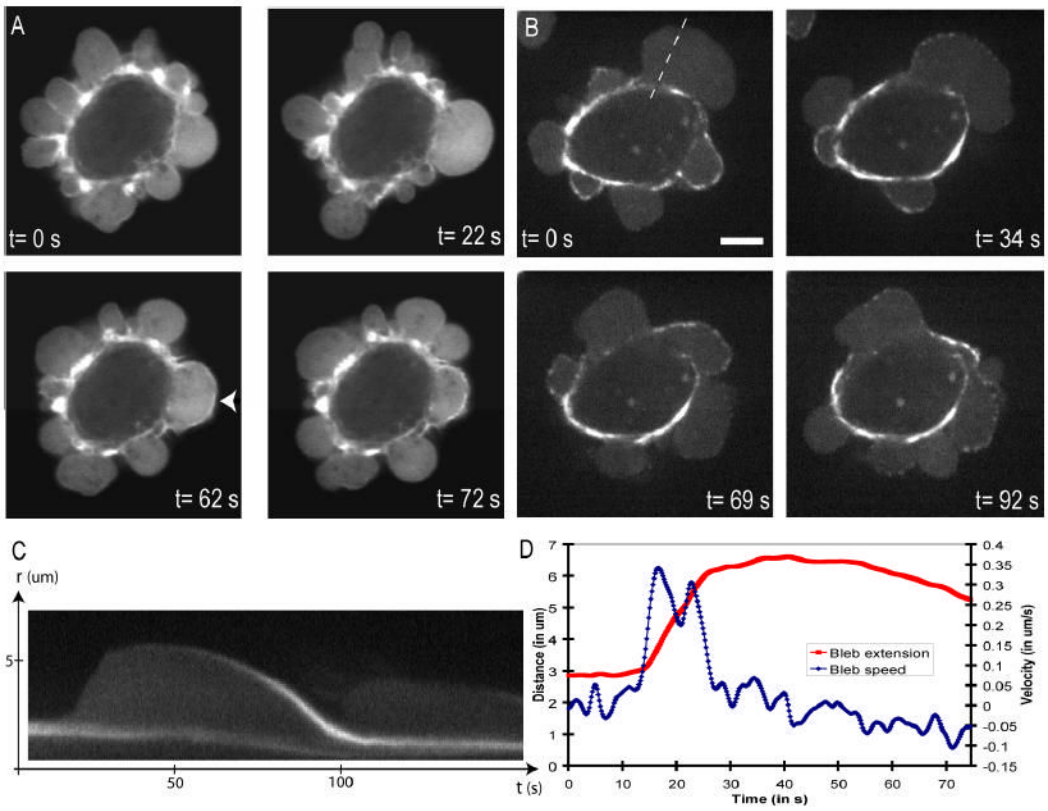

Figure 1.

Localisation of GFP-actin and GFP-MRLC in blebs shows that expansion is a passive process and retraction an active process necessitating actin and MRLC. All images were acquired by confocal microscopy. Scale bars=5 μm.

A. GFP-actin transfected cell. During bleb expansion, the bleb rim does not appear enriched in GFP-actin compared to the bleb interior (t=0s and t=22s). Once expansion has halted, an actin-rich rim forms at the bleb surface (t=62s, arrow head) and retraction begins. As retraction proceeds, the actin rim becomes wavy, suggesting that the cortex contracts as the bleb shrinks (t=72s).

B. GFP-MRLC transfected cell. Just after expansion has stopped, the bleb surface does not appear to be enriched in GFP-MRLC (t=0s). MRLC then accumulates in discrete foci (t=34s) and retraction starts (t=69s). As retraction ends, MRLC forms a continuum along the bleb rim (t=92s).

C. Kymograph of the expansion and retraction of the bleb in 1B (dashed line). As the bleb expands, there is no accumulation of MRLC at the bleb apex. As retraction proceeds, MRLC accumulates at the bleb.

D. Graph of the bleb extension and bleb velocity as a function of time for the bleb shown in 1C. The maximal bleb extension is ~3.5 μm (maximal speed of expansion ~0.35 $\mu m.s^{-1}$, speed of retraction ~0.1 $\mu m.s^{-1}$).

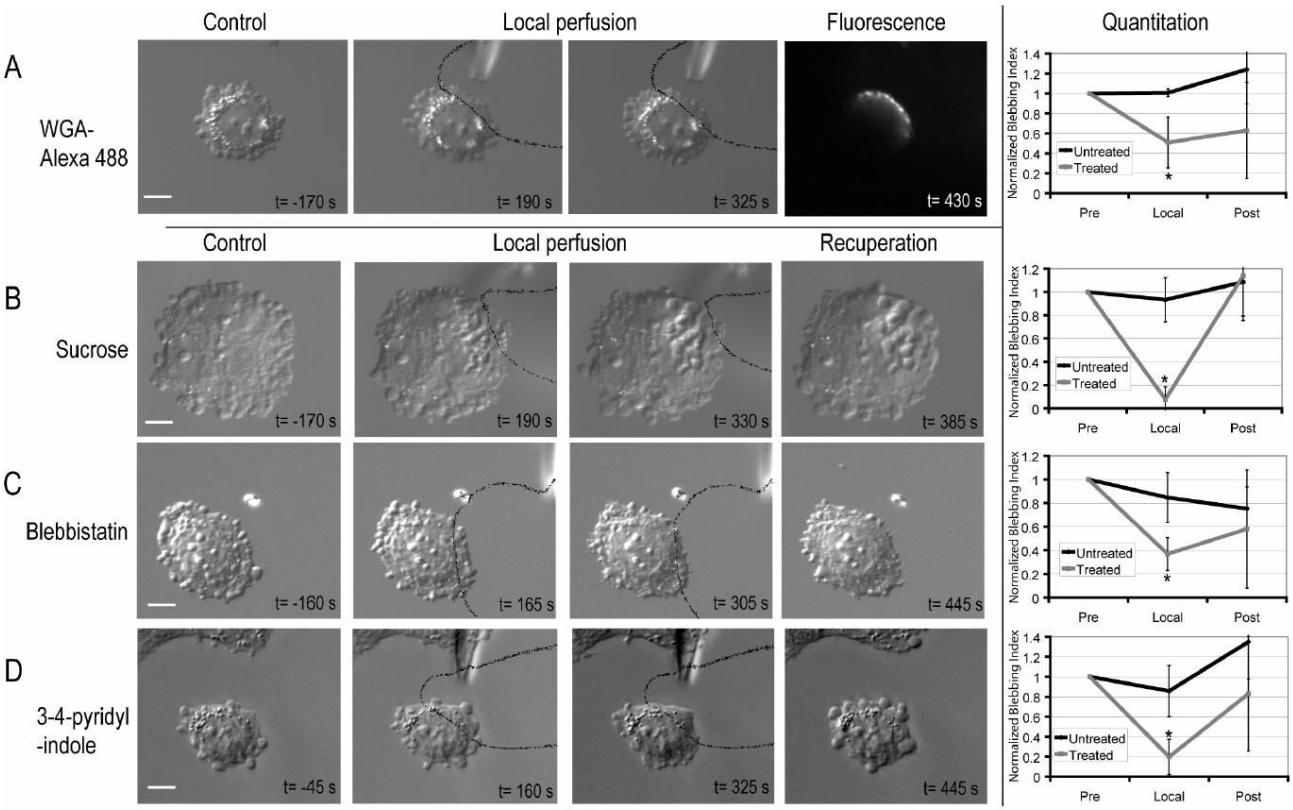

Figure 2.

Local perfusion can locally inhibit blebbing. In all cases, prior to application of treatment, the cells blebbed profusely around their periphery. Within 2–3 min of application, blebbing ceases in the area of application but continues undisturbed in the rest of the cell. In some cases, when the local perfusion was halted (t_{off}=350s in all cases), cells recovered and blebbed normally.

- **A.** Local perfusion of Wheat Germ Agglutinin (WGA) –Alexa 488. WGA-Alexa 488 was only incorporated in the region of the cell that was exposed to flow from the micropipette.
- **B.** Local perfusion of a 300mM sucrose solution. Vacuoles form in the vicinity of the perfused region.
- **C.** Local inhibition of myosin II ATP-ase by local perfusion of blebbistatin
- **D.** Local inhibition of ROCKI by 3-(4-pyridyl)indole. Solid black lines delineate the flow out of the micropipette. On each image, the inset text gives timing relative to local application of treatment. The normalised blebbing indices show the evolution over time of blebbing in the region exposed to inhibitor and in the free region. Error bars show the standard deviation. Asterisks denote significant changes in the blebbing index when compared to the initial blebbing index. Scale bars=10μm.

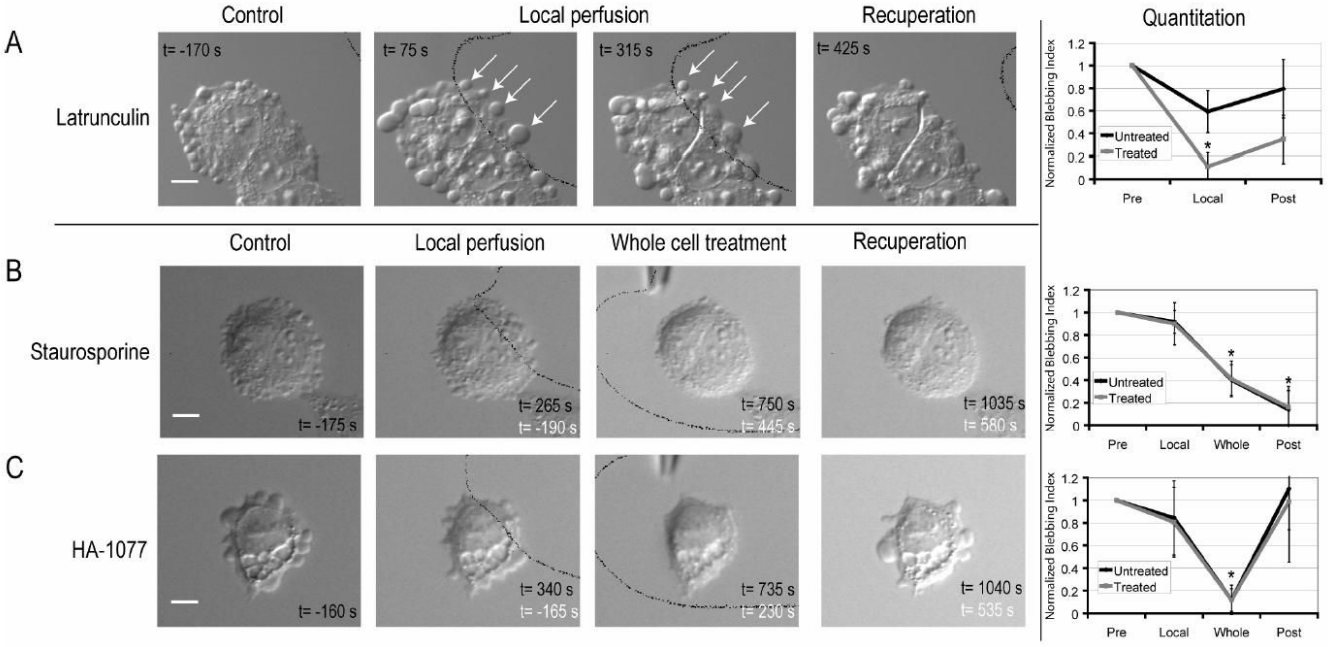

Figure 3.
Compounds with dual or global effects on blebbing.

- **A.** Local perfusion with Latrunculin B has a dual effect. When Latrunculin B is applied locally, bleb size increases globally (t=75s), and bleb dynamics cease in the treated area (t=75s, t=315s). Elsewhere, expansion and retraction continue.
- **B.** Global perfusion of Staurosporine is necessary to inhibit blebbing. Prior to perfusion (t=−170s) and after 395 s of local perfusion with Staurosporine, blebbing is unperturbed throughout the cell. When Staurosporine is applied to the whole cell (white letters, t=450s), blebbing ceases.
- **C.** Global perfusion of HA-1077 is necessitated to inhibit blebbing. After 340s of local HA-1077 application, blebbing is unperturbed. When the whole cell is exposed to inhibitor (t=230s, white letters), blebbing ceases. When perfusion is halted, blebbing is restored (t=535s, white letters).

Solid black lines delineate the flow coming out of the micropipette. Black text gives time relative to local application. White text gives time relative to global application. The normalised blebbing indices show the evolution over time of blebbing in the region exposed to inhibitor and in the free region. Error bars show the standard deviation. Asterisks denote significant changes in the blebbing index when compared to the initial blebbing index. Scale bars=10μm.

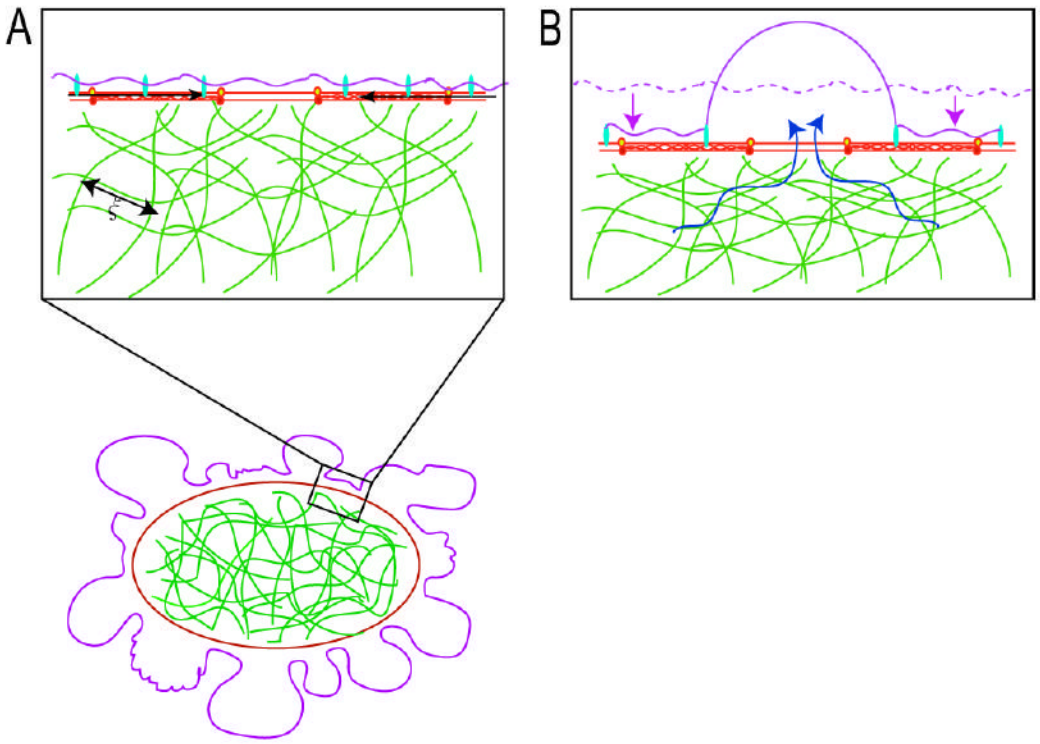

Figure 4.

Poroelastic description of blebbing. In all drawings, the actin cortex is drawn in red, the membrane is drawn in mauve, and the cytoskeletal meshwork is drawn in green.

A. In blebbing cells, a local contraction of the myosin II (black arrows) associated with the actin cortex leads to a shortening of the cortical periphery and therefore to a compression of the cytoskeletal network that fills the cell. The cytoskeletal network is porous and has an average pore size ξ. The compression of the cytoskeletal meshwork creates a hydrostatic pressure in the vicinity of the region of contraction and can lead to bleb nucleation and expansion.

B. Contraction of the actin cortex leads to a compression of the cytoskeletal network (the dashed mauve line indicates the original position of the cell surface) drives flow of cytosol in the opposite direction (blue arrows). If there is a local defect in membrane-cytoskeleton attachment, a bleb is extruded. Bleb expansion is opposed by two forces: extracellular osmotic pressure and membrane tension.